

5-Fluorouracil administration using clinical treatment protocol causes mucositis in the ileum in *Wistar* rats

A administração de 5-fluorouracil usando protocolo de tratamento clínico causa mucosite no íleo de ratos *Wistar*

La administración de 5-fluorouracilo mediante el protocolo de tratamiento clínico provoca mucositis en el íleon en ratas *Wistar*

Received: 10/26/2020 | Reviewed: 11/03/2020 | Accept: 11/04/2020 | Published: 11/08/2020

Lilian Catarim Fabiano

ORCID: <https://orcid.org/0000-0002-8905-5678>

Universidade Estadual de Maringá, Brasil

E-mail: lcatarim@hotmail.com

Mariana Conceição da Silva

ORCID: <https://orcid.org/0000-0001-6791-6898>

Universidade Estadual de Maringá, Brasil

E-mail: marianacsilva197@gmail.com

Karile Cristina da Costa

ORCID: <https://orcid.org/0000-0003-2334-2604>

Universidade Estadual de Maringá, Brasil

E-mail: karileccosta@gmail.com

Pedro Luiz Zonta de Freitas

ORCID: <https://orcid.org/0000-0003-0550-7524>

Universidade Estadual de Maringá, Brasil

E-mail: pedrolzf@hotmail.com

Camila Quaglio Neves

ORCID: <https://orcid.org/0000-0002-8466-4984>

Universidade Estadual de Maringá, Brasil

E-mail: camila_neves_76@hotmail.com

Stephanie Carvalho Borges

ORCID: <https://orcid.org/0000-0002-2534-143X>

Universidade Estadual de Maringá, Brasil

E-mail: stephaniecarvalhoborges@hotmail.com

Ana Cristina Breithaupt-Faloppa

ORCID: <https://orcid.org/0000-0003-0554-0674>

Universidade de São Paulo, Brasil

E-mail: abreithaupt@yahoo.com

Nilza Cristina Buttow

ORCID: <https://orcid.org/0000-0002-7228-7990>

Universidade Estadual de Maringá, Brasil

E-mail: ncbuttow@uem.br

Abstract

The present study evaluated the effects of 5-fluorouracil (5-FU) administration using a clinical treatment protocol for 14 days on the ileum in healthy *Wistar* rats. The animals were divided into two groups ($n = 6/\text{group}$): 5-FU-treated group and control group. The 5-FU group received 5-FU (15 mg/kg, i.p.) for 4 consecutive days, followed by a dose reduction to 6 mg/kg for 4 alternating days and then a last maintenance dose of 15 mg/kg on day 14. This treatment protocol is commonly used in the human clinical setting. The control group received saline (i.p.) according to the same treatment protocol. The ileum was then fractionated to evaluate oxidative stress parameters (catalase [CAT], superoxide dismutase [SOD], glutathione-S-transferase [GST], non-protein sulfhydryl groups [GSH], reactive oxygen species [ROS], and lipid hydroperoxide [LOOH]), markers of inflammation (interleukin-1 [IL-1], IL-6, myeloperoxidase [MPO], and N-acetylglucosaminidase [NAG]), and nitrite levels. HuC/D-immunoreactive myenteric neurons, neuronal nitric oxide synthase (nNOS)-immunoreactive nitrenergic neurons, and ileum wall morphometry were also analyzed. The 5-FU treatment protocol promoted oxidative stress and altered nitrite levels but did not cause inflammation. The treatment protocol also reduced the density of nitrenergic neurons and altered the morphometry of the general HuC/D-positive myenteric neuronal population and nNOS-positive nitrenergic neuronal subpopulation. Treatment with the clinical 5-FU treatment protocol promoted grade I mucositis in rats, characterized by oxidative stress and morphological changes in the intestinal wall.

Keywords: Oxidative stress; Inflammation; Myenteric plexus; Chemotherapy; Cancer.

Resumo

O estudo avaliou os efeitos da administração de 5-fluorouracil (5-FU) pelo protocolo de tratamento clínico por 14 dias no íleo em ratos *Wistar* saudáveis. Os animais foram divididos

em dois grupos (n = 6 / grupo): grupo tratado com 5-FU e grupo controle. O grupo 5-FU recebeu 5-FU (15 mg / kg, ip) por 4 dias consecutivos, com redução da dose para 6 mg / kg por 4 dias alternados, seguido de uma última dose de manutenção de 15 mg / kg no dia 14. Este protocolo é comumente usado no ambiente clínico humano. O grupo controle recebeu solução salina (i.p.) de acordo com o mesmo protocolo de tratamento. O íleo foi fracionado para avaliar os parâmetros de estresse oxidativo (catalase [CAT], superóxido dismutase [SOD], glutathione-S-transferase [GST], grupos sulfidril não proteicos [GSH], espécies reativas de oxigênio [ROS] e hidroperóxido de lipídio [LOOH]), marcadores de inflamação (interleucina-1 [IL-1], IL-6, mieloperoxidase [MPO] e N-acetilglucosaminidase [NAG]) e níveis de nitrito. Neurônios mioentéricos imunorreativos HuC / D, neurônios nitrérgicos imunorreativos de óxido nítrico neuronal (nNOS) e morfometria da parede do íleo também foram analisados. O tratamento com 5-FU promoveu estresse oxidativo e alterou os níveis de nitrito, mas não causou inflamação. Também reduziu a densidade de neurônios nitrérgicos e alterou a morfometria da população geral de neurônios mioentéricos HuC / D positivo e da subpopulação de neurônios nitrérgicos positivos para nNOS. O tratamento com protocolo clínico de 5-FU promoveu mucosite grau I em ratos, caracterizada por estresse oxidativo e alterações morfológicas na parede intestinal.

Palavras-chave: Estresse oxidativo; Inflamação; Plexo mioentérico; Quimioterapia; Câncer.

Resumen

Este estudio evaluó la administración de 5-fluorouracilo (5-FU) por el protocolo de tratamiento clínico durante 14 días en el íleon en ratas *Wistar* sanas. Los animales se dividieron en dos grupos (n = 6 / grupo): grupo tratado con 5-FU y grupo control. El grupo de 5-FU recibió 5-FU (15 mg / kg, ip) durante 4 días consecutivos, 6 mg / kg durante 4 días alternos, seguida de una última dosis de mantenimiento de 15 mg / kg en el día 14. Este protocolo se usa comúnmente en el entorno clínico humano. El grupo de control recibió solución salina (i.p.) con el mismo protocolo de tratamiento. Fueron evaluados los parámetros de estrés oxidativo (catalasa [CAT], superóxido dismutasa [SOD], glutatión-S-transferasa [GST], grupos sulfhidrilo no proteicos [GSH], especies reactivas de oxígeno [ROS] e hidroperóxido de lípido [LOOH]), marcadores de inflamación (interleucina-1 [IL-1], IL-6, mieloperoxidasa [MPO] y N-acetilglucosaminidasa [NAG]) y niveles de nitrito, se analizaron las neuronas mientéricas inmunorreactivas de HuC / D, las neuronas nitrérgicas inmunorreactivas del óxido nítrico neuronal (nNOS) y la morfometría de la pared del íleon. El tratamiento con 5-FU promovió el estrés oxidativo y alteró los niveles de nitrito, pero no

provocó inflamación. Redujo la densidad de neuronas nitrérgicas, alteró la morfometría de la población general de neuronas mientéricas positivas para HuC / D y la subpoblación de neuronas nitrérgicas positivas para nNOS. El tratamiento con un protocolo clínico de 5-FU promovió mucositis grado I en ratas, caracterizada por estrés oxidativo y cambios morfológicos en la pared intestinal.

Palabras clave: Estrés oxidativo; Inflamación; Plexo mientérico; Quimioterapia; Cáncer.

1. Introduction

Cancer is the second leading cause of death worldwide (Organization, 2018). Data from the International Association of Cancer Registries estimate that 11,454,037 new cases of cancer will occur by 2040, which is 6,833,432 more deaths than in 2018. Solid cancers are the most frequent type of cancer, such as breast, prostate, lung, and colorectal (Ferlay et al., 2018). Several types of treatments have been used, but most of them have high costs (e.g., immunotherapy, hormone therapy, targeted therapy, chemotherapy, and radiation therapy). One of the least expensive and most efficient treatments for solid cancers is 5-fluorouracil (5-FU) antimetabolite chemotherapy. It acts by inhibiting the enzyme thymidylate synthase, which plays a key role in DNA synthesis. 5-Fluorouracil promotes changes in DNA and RNA, leading to cell death (Cuéllar-Garduño, 2015). However, 5-FU is not selective for cancer cells; it also attacks healthy cells, which can trigger serious side effects. Mucositis is a common side effect of this drug, which affects up to 40% of patients (Harris, 2006) and causes severe pain and discomfort, episodes of vomiting, changes in the structure of the intestinal wall, and changes in gastrointestinal transit, which can compromise patients' nutritional status and quality of life (Gelen et al., 2018; Soares et al., 2008).

Most studies of 5-FU that evaluated its effects on the gastrointestinal tract used a single high dose (El-Sayyad et al., 2009; Leocádio et al., 2015; Medeiros et al., 2018; Soares et al., 2008). Such a model differs from conventional clinical treatment in human patients, in which the prescribed dose of 5-FU is based on the patient's body weight. Thus, little is known about the effects of this clinical treatment protocol on intestinal mucosa.

Studies of high doses of 5-FU using various treatment protocols have shown significant changes in several parameters, such as oxidative stress (Leocádio et al., 2015) inflammation (Leocádio et al., 2015; Medeiros et al., 2018), mucositis (Soares et al., 2008), and morphology of the intestinal wall (Leocádio et al., 2015) and myenteric plexus (El-Sayyad et al., 2009). However, such alterations do not necessarily reflect the clinical protocol

that is used to treat cancer. Knowledge of changes in the intestinal mucosa that are caused by the human treatment regimen is useful for discovering alternative therapeutic approaches to alleviate complications and improve quality of life.

The present study evaluated parameters of oxidative stress and inflammation and morphology of the intestinal wall and myenteric plexus in the ileum in Wistar rats that were treated with a clinical 5-FU treatment protocol for 14 days.

2. Methodology

2.1 Animals and experimental protocol

Twelve male Wistar rats (270.6 ± 8.2 g) were obtained from the central vivarium of the State University of Maringá and housed in the vivarium in the Department of Morphological Sciences, State University of Maringá. The animals were housed at a controlled temperature ($22^{\circ}\text{C} \pm 2^{\circ}\text{C}$) under a 12 h/12 h light/dark cycle with *ad libitum* access to water and standardized rodent chow (NUVILAB, recommended by the National Research Council and National Institutes of Health, USA). The study was approved by the Ethics Committee on the Use of Animals of the State University of Maringá (CEUA no. 4422140918). All analyzes performed in this experiment are quantitative in nature (Pereira et al., 2018).

The animals were assigned to two groups ($n = 6/\text{group}$): 5-FU-treated group and control group. The 5-FU group received 5-FU (15 mg/kg, i.p.) for 4 consecutive days, followed by a dose reduction to 6 mg/kg for 4 alternating days and a last maintenance dose of 15 mg/kg on day 14, based on the protocol that is recommended by the manufacturer (Fluorouracil, Neugrast) for human clinical treatment. The control group received saline (i.p.) according to the same treatment protocol as the 5-FU group. The animals were fasted for 12 h after the last injection before euthanasia.

2.2 Organ collection

On day 15, the animals were sacrificed by a lethal dose of sodium thiopental (120 mg/kg, i.p.; Cristália, Produtos Químicos Farmacêuticos, São Paulo, SP, Brazil). The distal ileum was collected and fractionated to analyze biochemical markers of oxidative stress, markers of inflammation, and total protein levels and to perform histological and

immunofluorescence analyses of neuronal populations. The samples of the ileum were stored at -80°C for the biochemical analyses.

2.3 Sample preparation

The ileum was weighed and homogenized in potassium phosphate buffer (200 mM, pH 6.5) in a 3:1 ratio to obtain the homogenate. A portion of the homogenate was used to evaluate reduced glutathione (GSH) levels, and the remainder was centrifuged at 9000 rotations per minute for 20 min. The resulting supernatant was used to detect superoxide dismutase (SOD), catalase (CAT), glutathione-S-transferase (GST), and lipid hydroperoxide (LOOH). The pellet was used to detect myeloperoxidase (MPO) and N-acetylglucosaminidase (NAG).

2.3.1 Total proteins

Protein levels in the supernatant were evaluated using the BCA Protein Assay Kit (Pierce Biotechnology, Rockford, IL, USA). Readings were performed using a 96-well plate in a spectrophotometer at 462 nm.

2.3.2 Levels of GSH and LOOH

To measure GSH levels, the tissue was homogenized in 200 mM phosphate buffer (pH 6.5), and 25% trichloroacetic acid was added to the homogenate for protein precipitation. 5,5'-Dithiobis-2-nitrobenzoic acid (10 mM) was then added according to the protocol of Sedlak and Lindsay (Sedlak & Lindsay, 1968). The reaction was read on a spectrophotometer at a wavelength of 415 nm. The values were interpolated on a standard GSH curve and are expressed as µg GSH/g tissue.

To measure LOOH levels, the homogenate was centrifuged, and a portion of the supernatant was used for the iron II oxidation test in the presence of orange xylenol as described by Jiang (Jiang et al., 1991). Readings were performed on a spectrophotometer at a wavelength of 560 nm. The results are expressed as mmol/mg of tissue.

2.3.3 Enzymatic activity of SOD, CAT, and GST

The activity of SOD was evaluated according to the protocol of Marklund and Marklund (Marklund & Marklund, 1974), based on its ability to inhibit the autooxidation of pyrogallol. Readings were performed on the spectrophotometer at a wavelength of 405 nm. The results are expressed as units (U) of SOD/mg of protein. The activity of CAT was analyzed by adding a supernatant solution that contained 30% H₂O₂ and 0.4 M Tris-HCL buffer (pH 8.5) according to Aebi (Aebi, 1984). Readings were performed at a wavelength of 240 nm over 5 min. The results are expressed as mmol/min/mg of protein. To analyze GST activity, 3 mM 1-chloro-2,4-dinitrobenzene that contained 3 mM GSH was added to potassium phosphate buffer according to the method of Warholm et al. (Warholm et al., 1985). Kinetics were read on the spectrophotometer at a wavelength of 340 nm. The results are expressed as mmol/min/mg of protein.

2.3.4 Reactive oxygen species

Reactive oxygen species were assessed according to Keston and Brandt (1965) (Brandt & Keston, 1965). The test consisted of the oxidation of the fluorescent probe dichlorofluorescein (DCFH) by ROS and reactive nitrogen species. The samples of the ileum were used to prepare the homogenate. The samples were weighed to approximately 200 mg and homogenized in 1 ml of sodium phosphate buffer (0.08 M, pH 7.5). The homogenate was incubated with 1 mM DCFH for 40 min in the dark. After incubation, fluorescence was measured in a spectrofluorimeter using a microplate at an excitation wavelength of 488 nm and emission wavelength of 520 nm.

2.3.5 Enzymatic activity of myeloperoxidase MPO and NAG

After centrifuging the homogenates, the pellet was resuspended with 80 mM potassium phosphate buffer in the presence of 0.5% hexadecyltrimethylammonium. The sample was centrifuged again, and the supernatant was added to tetramethylbenzidine. The enzymatic activity of MPO was read in a spectrophotometer at 620 nm. The results are expressed as the optical density (OD)/min/mg of protein. For the analysis of NAG, the pellet was resuspended and centrifuged again. The supernatant was added to a 96-well microplate with 50 mM citrate buffer (pH 4.5) and 2.24 mM 4-nitrophenyl-*N*-acetyl- β -D-glucosamine

solution and then incubated at 37°C for 60 min. The reaction was stopped with 200 mM glycine buffer (pH 10.4). Readings were performed on a spectrophotometer at a wavelength of 405 nm. The results are expressed as OD/min/mg of protein.

2.4 Nitrite quantification

To indirectly quantify nitric oxide levels, we measured its byproduct nitrite using the Griess reaction technique, adapted from Tiwari et al. (Tiwari et al., 2011). A portion of the ileum was homogenized in 0.1 M phosphate-buffered saline (PBS; pH 7.4) and centrifuged. The supernatant and Griess solution (phosphoric acid, sulfanilamide, and *N*-1-naphthalylethylenediamide) were added to a 96-well plate, and absorbance was read in a spectrophotometer at a wavelength of 570 nm. A standard curve was made using dilutions of NaNO₂ from 100 to 1.56 μM. Nitrite levels are expressed as μM.

2.5 Interleukin-1 and IL-6 levels

The tissue samples were centrifuged, and IL-1 and IL-6 concentrations were determined in 96-well plates using an enzyme-linked immunosorbent assay (R&D Systems) according to the manufacturer's instructions.

2.6 Histological analysis

A portion of the ileum was fixed in 4% paraformaldehyde (pH 7.4) for 6 h, dehydrated in a series of alcohol, and cleared in xylol. The samples were embedded in paraffin and cut into semi-serial sections (5 μm) using a microtome. The material was separated to perform hematoxylin and eosin (H&E) and periodic acid Schiff (PAS) staining according to McManus (McManus, 1946). Images of slides that were stained with H&E were captured under an optical microscope (10× magnification) using an image capture system and a high-resolution camera. Fifty measurements were taken for each of the structures of the ileum (total wall, height and width of villi, depth of crypts, and thickness of the submucosa and muscular tunic). Goblet cells were quantified on slides that were stained with PAS under an optical microscope. A total of 2,500 epithelial cells were counted, and the goblet cell index was calculated.

2.7 Immunofluorescence

A portion of the ileum was washed in 0.1 M PBS (pH 7.4) and fixed in 4% paraformaldehyde (pH 7.4) for 3 h. The sample was then washed in PBS and refrigerated in PBS solution with 0.08% sodium azide. The segment was dissected with tweezers under a stereomicroscope to separate the muscular and submucosal tunics.

2.7.1 HuC/D-immunoreactive myenteric neurons and nNOS-immunoreactive nitrergic neurons

Whole-mount preparations of the muscular tunic were subjected to immunofluorescence to mark the general population of myenteric neurons (HuC/D⁺) and subpopulation of nitrergic neurons (nNOS⁺). Each membrane was washed three times with PBS-T (0.1 M PBS [pH 7.4] and 0.5% Triton X-100) for 10 min each, followed by 2 h of incubation in blocking solution (3% bovine serum albumin [BSA] and 20% donkey serum in PBS-T). Afterward, the membranes were double labeled using primary anti-HuC/D antibody (1:400, mouse, Invitrogen, Eugene, OR, USA, catalog no. A21271) and primary anti-nNOS antibody (1:400, rabbit, Invitrogen, Eugene, OR, USA, catalog no. 617000) at room temperature for 48 h. The incubation medium was composed of PBS-T, 2% BSA, and 2% donkey serum. After incubation, the membranes were washed three times with PBS-T for 10 min each and incubated in secondary anti-mouse antibody (1:400, Alexa Fluor 568, Molecular Probes, Invitrogen, Eugene, OR, USA, catalog no. A10037) and secondary anti-rabbit antibody (1:400, Alexa Fluor 488, Molecular Probes, Invitrogen, Eugene, OR, USA, catalog no. A21206) for 2 h in the dark. The incubation medium contained PBS-T, 2% BSA, and 2% donkey serum. The membranes were washed four times for 10 min each and mounted on glass slides with Prolong Gold Antifade (Life Technologies do Brasil Com. Ind. Prod. Biotec. Ltda, São Paulo, SP, Brazil) and refrigerated while protected from light.

2.7.2 Quantification of HuC/D-immunoreactive myenteric neurons and nNOS-immunoreactive nitrergic neurons

Thirty images of the whole-mount slides were captured using an Olympus FSX100 fluorescence microscope. The images were analyzed using ImagePro Plus software (v. 4.5.029, Media Cybernetics, Silver Spring, MD, USA). All neurons that were present in the

30 images were counted under a 20× objective. The area of each image was approximately 0.136 mm², and the total quantified area was 4.066 mm². The results are expressed as the number of neurons/cm².

2.7.3 Morphometric analysis of HuC/D-immunoreactive myenteric neurons and nNOS-immunoreactive nitrenergic neurons

The morphometric analysis was performed using images that were captured at 20× magnification and analyzed using ImagePro Plus software (v. 4.5.029, Media Cybernetics, Silver Spring, MD, USA). The profiles of 100 cell bodies of HuC/D- and nNOS-immunoreactive neurons (expressed as μm²) from each animal were measured.

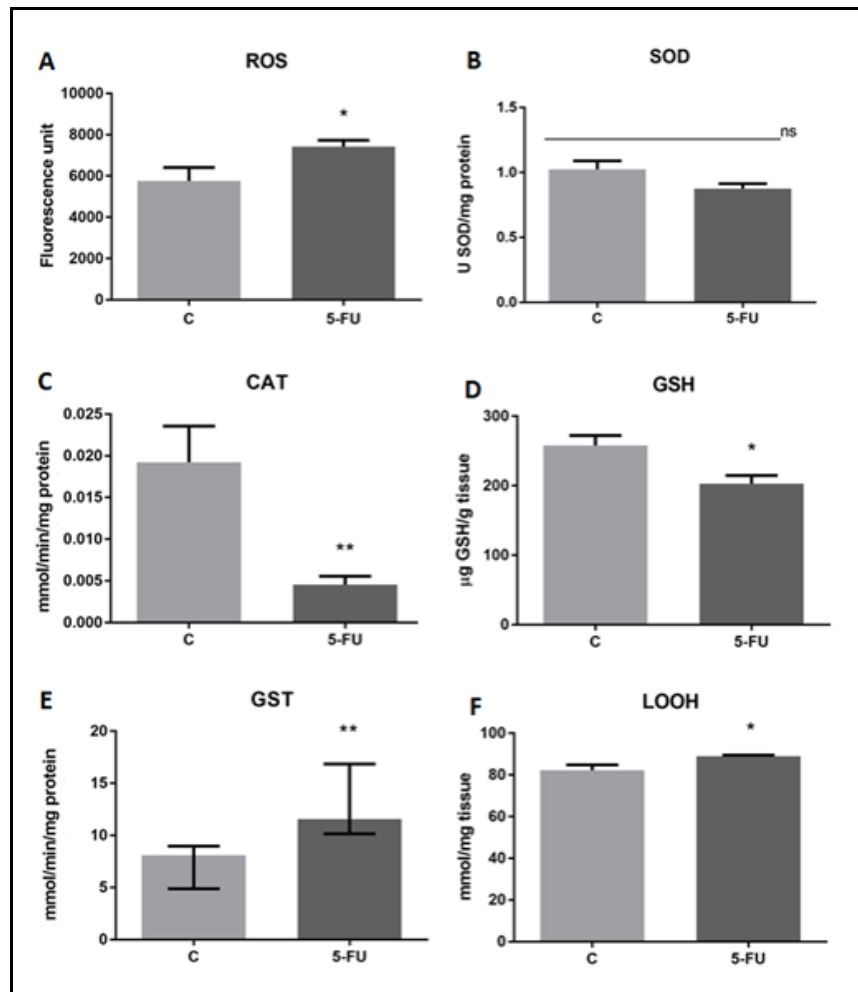
2.8 Statistical analysis

The statistical analysis was performed using GraphPad Prism 7.05 software. For groups with a normal data distribution, Student's *t*-test was performed. The Mann-Whitney test was used for nonparametric data. Parametric data are expressed as the mean ± standard error of the mean. Nonparametric data are expressed as the median ± confidence interval. Values of *p* < 0.05 were considered statistically significant.

3. Results

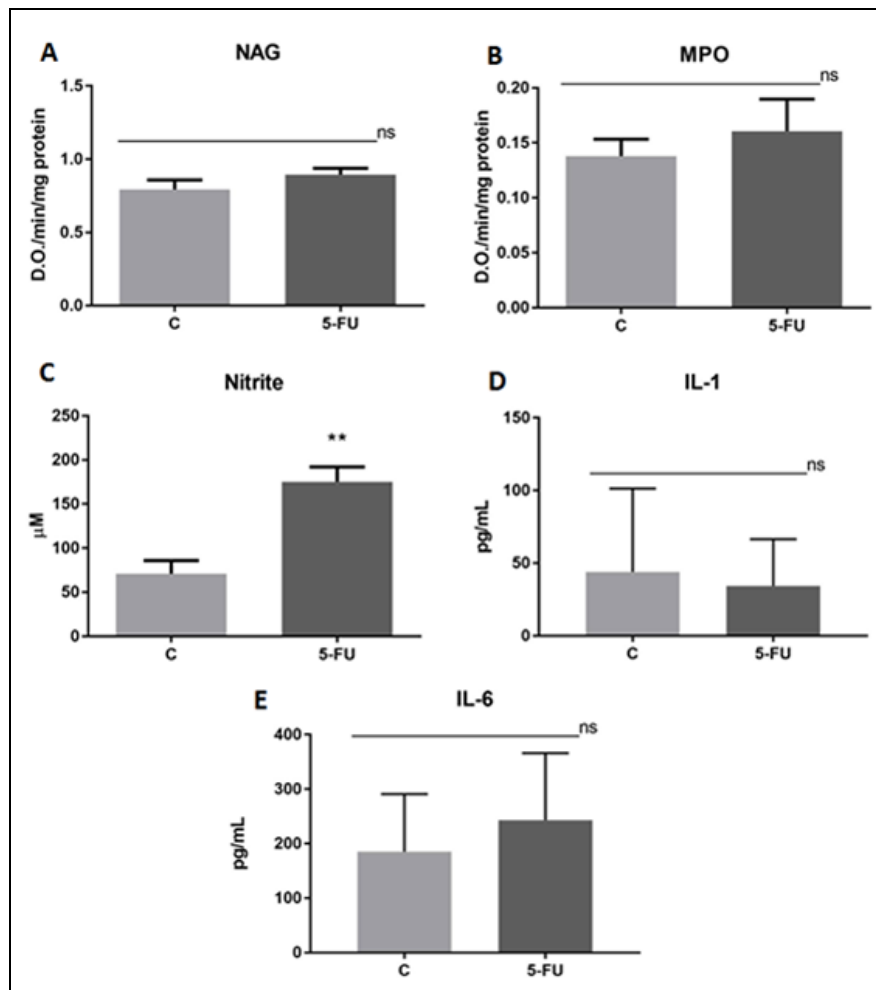
Fig. 1 and 2 show the results of the biochemical analysis of the rat ileum. A significant increase in ROS levels was observed in the 5-FU group compared with the control group (*p* < 0.05). Activity of the CAT enzyme (*p* < 0.01) and GSH levels (*p* < 0.05) significantly decreased in the 5-FU group compared with the control group. Activity of the GST enzyme (*p* < 0.01), LOOH levels (*p* < 0.05), and nitrite levels (*p* < 0.01) significantly increased in the 5-FU group compared with the control group. No significant differences in the activity of SOD, MPO, or NAG or the levels of IL-1 and IL-6 were found between the 5-FU and control groups (*p* > 0.05).

Figure 1 - Biochemical assays of oxidative stress parameters.



Note. (A) reactive oxygen species (ROS), (B) superoxide dismutase (SOD) activity, (C) catalase (CAT) activity, (D) non-protein sulfhydryl groups (GSH) levels, (E) glutathione-S-transferase (GST) activity, and (F) lipid hydroperoxide (LOOH) levels. Parametric data are expressed as the mean \pm standard error of the mean. Nonparametric data are expressed as the median \pm confidence interval (E). * $p < 0.05$, ** $p < 0.01$. Source: Authors.

Figure 2 - Biochemical assay of inflammatory parameters.



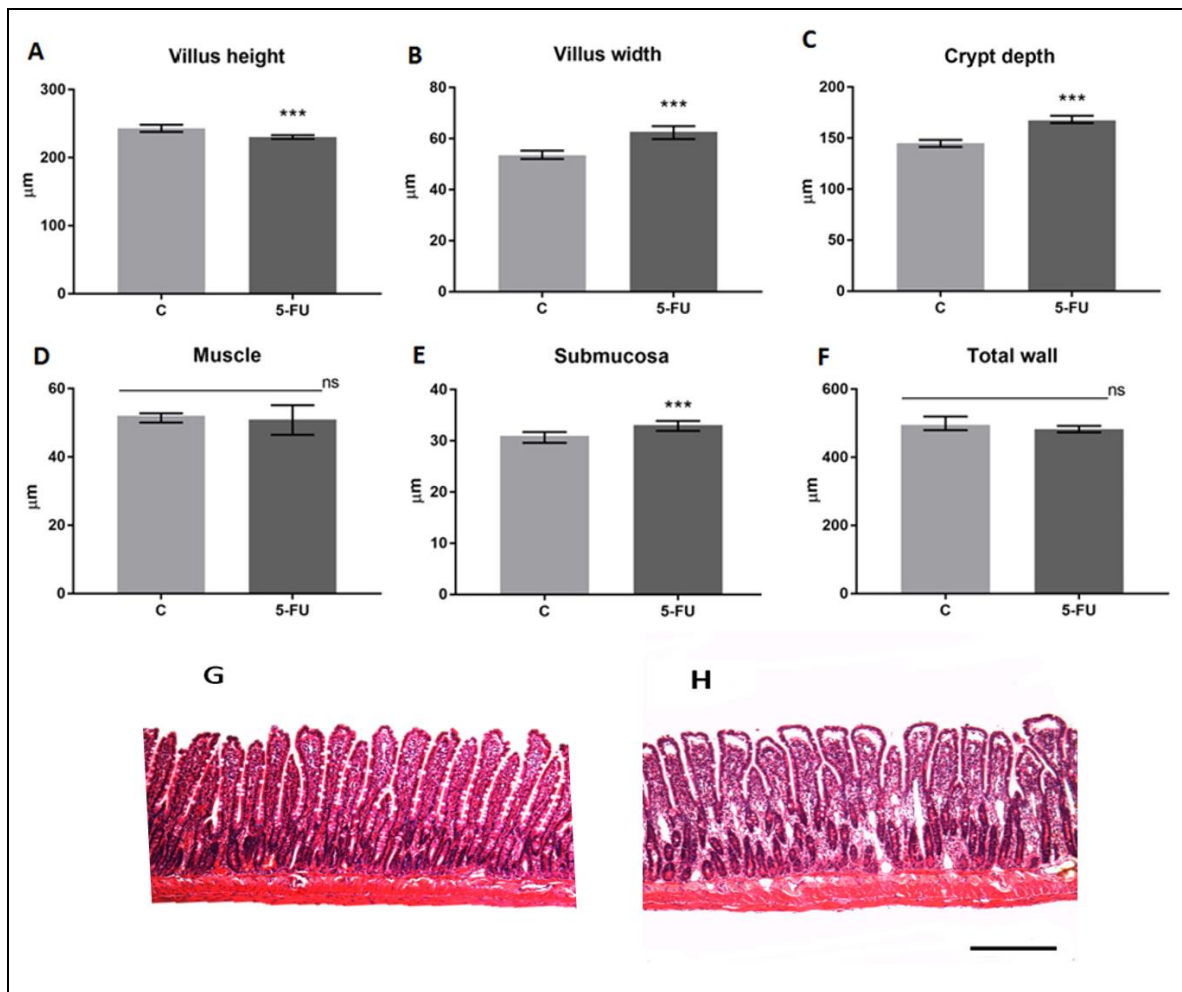
Note. (A) N-acetylglucosaminidase (NAG) activity, (B) myeloperoxidase (MPO) activity, (C) nitrite levels, (D) IL-1 levels, and (E) IL-6 levels. Parametric data are expressed as the mean \pm standard error of the mean. ** $p < 0.01$. Source: Authors.

3.2 Analysis of histological parameters

3.2.1 Ileum wall

Fig. 3 shows the morphometry of the ileum wall. Villus height significantly decreased ($p < 0.001$) and villus width, crypt depth, and submucosa thickness significantly increased ($p < 0.0001$) in the 5-FU group compared with the control group. No differences in the total wall and muscle tunic measurements were found between groups.

Figure 3 - Analysis of the morphometry of the ileum wall.



Note. (A) villus height, (B) villus width, (C) crypt depth, (D) muscle tunica thickness, (E) submucosa thickness, and (F) total wall thickness. (G, H) Photomicrographs of the ileum wall in the control group (G) and 5-FU group (H). Scale bar = 200 µm. Nonparametric data are expressed as the median ± confidence interval. *** $p < 0.001$. Source: Authors.

3.2.2 Goblet cells

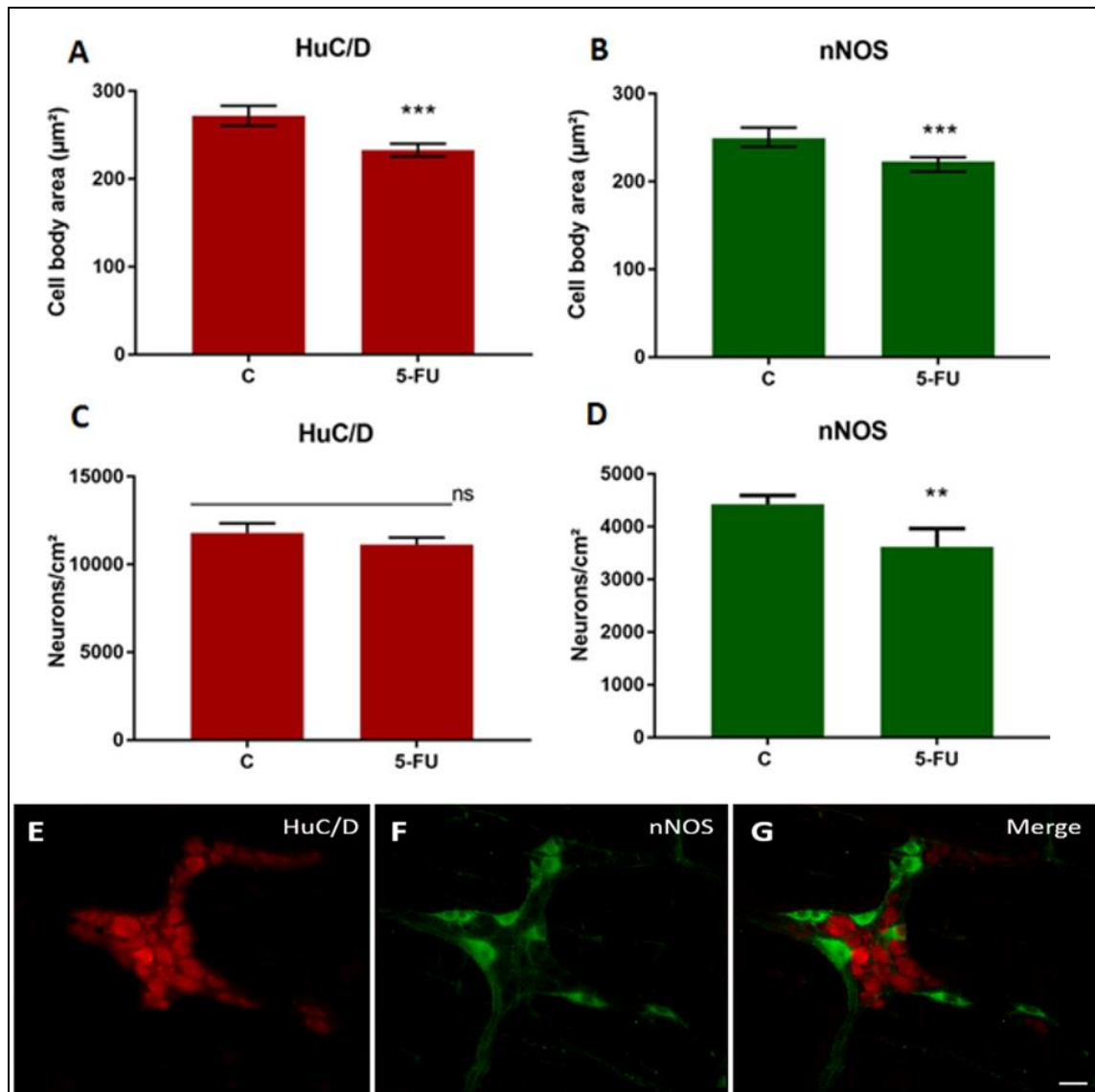
The goblet cell index was significantly lower in the 5-FU group (17.06 ± 0.60) compared with the control group (19.7 ± 0.52 ; $p < 0.05$).

3.3 Density and morphometry of myenteric neurons

The morphometric analysis showed significant decreases in the cell body area of the two neuronal populations in the 5-FU group compared with the control group ($p < 0.001$). A significant decrease in the density of nNOS-immunoreactive nitrergic neurons was observed in the 5-FU group compared with the control group ($p < 0.01$). No differences in the HuC/D-

immunoreactive general neuronal population were found between groups (Fig. 4).

Figure 4 - Mean neuronal cell body area (μm^2) of the HuC/D-positive general neuronal population



Note. (A) and nNOS-positive nitroergic subpopulation (B), density (neurons/cm²) of the general neuronal population (C), and density of the nitroergic subpopulation (D). Photomicrographs show the immunofluorescence of myenteric neurons that were immunoreactive to HuC/D (E), nNOS (F), and double labeling of HuC/D⁺ and nNOS⁺ (G). Scale bar = 50 μm . Parametric data are expressed as the mean \pm standard error of the mean. Nonparametric data are expressed as the median \pm confidence interval. *** $p < 0.001$. Source: Authors.

4. Discussion

The use of chemotherapeutic drugs is associated with various side effects that can impair the quality of life of cancer patients. Several studies have investigated the effects and

consequences of chemotherapy, but the experimental treatment protocols that are used in these studies often differ substantially from clinical practice. In the present study, we employed a clinical treatment protocol. Our results were consistent with the development of stage I mucositis. Five stages are used to describe the pathogenesis of mucositis according to the degree of injury (Sonis et al., 2004). Stage I is characterized by the presence of ROS and oxidative stress and their harmful cellular effects on the mucosa and submucosa. Stage II is characterized by the upregulation and generation of messenger signals that reflect high levels of oxidative stress and the production of proinflammatory cytokines, such as nuclear factor κ B, tumor necrosis factor α , IL-1, and IL-6. Stage III is characterized by even higher levels of these proinflammatory cytokines. Stage IV is characterized by ulcerations and loss of integrity of the epithelial barrier that allows the entry of toxic and pathogenic agents and the recruitment of tissue macrophages. Stage V is characterized by a healing process that is associated with tissue restoration (Sonis et al., 2004).

In the present study, we observed a significant 28% increase in ROS generation and 8% increase in LOOH levels. 5-Fluorouracil generates ROS that can trigger oxidative stress (Kang et al., 2014; Sonis et al., 2004). Reactive oxygen species are highly toxic and can damage cellular structures, such as nucleic acids, lipids, and proteins (Birben et al., 2012). Oxidative stress that is caused by chemotherapy can cause irreversible damage to DNA, cell damage, and blood vessel injury, generating a cascade of biological changes (Sonis et al., 2004). These changes are essential for the beneficial effects of these drugs against tumors, but healthy tissues can also be negatively impacted, compromising patients' quality of life. To mitigate damage that is caused by chemotherapy-induced ROS production, activity of the endogenous antioxidant defense system is amplified to maintain homeostasis (Muthu et al., 2013; Rtibi et al., 2018). This defense mechanism depends on combined actions of enzymatic and non-enzymatic antioxidant molecules (Birben et al., 2012). Various parameters are used to evaluate oxidative stress, including the activity of SOD, CAT, and GST, levels of GSH, and the formation of ROS and LOOH. In the present study, treatment with a routine clinical dose of 5-FU did not alter SOD activity. However, 5-FU at this dose decreased CAT activity by 23%. This result was also observed in previous studies that tested a higher dose of 5-FU (100 mg/kg) (Muthu et al., 2013; Rtibi et al., 2018), contributing to a state of oxidative stress, in which the antioxidant enzyme CAT, under normal conditions, reduces H_2O_2 to H_2O and O_2 to prevent oxidative damage (Birben et al., 2012). The GSH tripeptide acts by removing free radicals, which may contribute to the reduction of lipid peroxidation (Birben et al., 2012).

The action of GST can be observed after the use of xenobiotics, including

chemotherapeutic agents. An increase in GST activity indicates an attempt by the body to lower the cytotoxicity of these drugs (Prabhu et al., 2004). Reduced glutathione also acts as a cofactor by donating electrons to GST. Therefore, increases in GST may be related to decreases in GSH (Shiota et al., 2010; Sies, 1999). In the present study, we observed a 21% reduction of GSH levels. In a previous study (Soares et al., 2008), treatment with a single dose of 5-FU (150 mg/kg) decreased GSH levels in the ileum on day 1. After day 3 of treatment, decreases in GSH levels were present throughout the extension of the small intestine (Soares et al., 2008), with a 6% increase in GST activity.

We also found a significant increase in nitrite levels in the ileum wall. The levels of nitrite (i.e., a byproduct of nitric oxide) were assessed using the Griess technique. Excess nitric oxide can cause cellular and tissue damage (Kubes & McCafferty, 2000). When nitric oxide combines with the hydroxyl radical (OH•), it promotes formation of the peroxynitrite radical (ONOO⁻), a powerful oxidizing agent (Rivera et al., 2011).

In stage II and III mucositis, inflammation is observed. In studies of high-dose 5-FU, an increase in the proinflammatory cytokines IL-1 and IL-6 was observed (50 mg/kg 5-FU) (Medeiros et al., 2018), and an increase in MPO and NAG activity was observed (200 mg/kg 5-FU) (Leocádio et al., 2015), indicating a high degree of mucositis. In the present study, we did not observe significant changes in the expression of IL-1 or IL-6 or the activity of MPO and NAG, which are indirect markers of tissue inflammation. These results indicated that the clinical treatment protocol with lower doses of 5-FU that was used in the present study did not promote an inflammatory process in the intestine.

In addition to assessing oxidative stress and inflammatory parameters, we also evaluated morphological changes in the intestinal wall to further characterize mucositis (Sonis et al., 2004). 5-Fluorouracil does not distinguish between cancer cells and normal cells, instead globally attacking cells that are characterized by rapid growth and division (El-Sayyad et al., 2009). Even at lower doses of 5-FU, our results were similar to other studies with regard to the morphology of the intestinal mucosa. Studies that tested single doses of 100 (Chang et al., 2012) and 450 mg/kg (Soares et al., 2013) also reported changes in the intestinal mucosa, such as a decrease in villus height and an increase in crypt depth. Other authors suggested that mucosal damage that is caused by 5-FU is associated with ROS generation (Okumura & Takeda, 2017; Rtibi et al., 2018; Shiota et al., 2010). A decrease in villus height was observed at a 5-FU dose of 300 mg/kg (Shiota et al., 2010), and the formation of abscesses and destruction of crypts were observed at doses of 100 (Rtibi et al., 2018) and 50 mg/kg (Yasuda et al., 2013). Furthermore, a decrease in villus length was

observed at the 50 mg/kg dose (Yasuda et al., 2013). The administration of 23 mg/kg 5-FU three times weekly for 2 weeks resulted in a reduction of goblet cells (McQuade et al., 2016). In the present study, our treatment regiment with clinical doses of 5-FU caused a 13% reduction of goblet cells. Goblet cells serve as a physical and chemical barrier to the mucosa, ensuring protection and preventing intestinal inflammation (Okumura & Takeda, 2017). The reduction of mucus production by goblet cells can lead to intestinal barrier dysfunction. In patients with inflammatory bowel disease, for example, a reduction of the mucus layer that covers the mucosa has been observed, rendering it susceptible to invasion by microorganisms (Okumura & Takeda, 2017). Thus, even at lower doses, 5-FU altered the histology of the ileum wall (Costa et al., 2019; El-Sayyad et al., 2009; Sies, 1999).

We also observed changes in neurons in the myenteric plexus. Treatment with 5-FU using the clinical protocol significantly decreased the density (by 18%) and morphometry (by 10%) of nNOS-positive nitrergic neurons. Although the density of the general neuronal population (HuC/D-positive) did not decrease, we observed a significant 14% reduction of the morphometry of these neurons. (McQuade et al., 2016) reported a reduction of the density of nNOS-positive nitrergic neurons after 2 weeks when 23 mg/kg 5-FU was administered three times weekly. These authors also found a reduction of the density of the PGP9.5-positive general neuronal population. Costa et al. (Costa et al., 2019) reported that a single dose of 450 mg/kg 5-FU reduced the density of HuC/D-positive neurons. These findings indicate that higher doses of 5-FU cause neurotoxicity, with more exacerbated changes in intestinal motility that can compromise patients' quality of life (Soares et al., 2008).

5. Final Considerations

In summary, 5-FU treatment using a clinical protocol promoted oxidative stress, caused histological changes in the ileum wall, and altered the general population and nitrergic subpopulation of myenteric plexus neurons but did not cause inflammation. Thus, this treatment protocol that is used in the clinical setting appears to cause stage I mucositis, which can lower the quality of life of cancer patients. These findings elucidate changes that occur in the gastrointestinal tract during 5-FU chemotherapy and may contribute to the discovery of other molecules and compounds that may mitigate the side effects of 5-FU. But further studies are needed to assess the effect of the 5-FU clinical treatment protocol on tissues with the presence of a tumor.

References

- Aebi, H. (1984). Catalase in Vitro: Methods in Enzymology. *Academic Press*, 121-26. [https://doi.org/10.1016/S0076-6879\(84\)05016-3](https://doi.org/10.1016/S0076-6879(84)05016-3)
- Birben, E., Sahiner, U. M., Sackesen, C., Erzurum, S., & Kalayci, O. (2012). Oxidative stress and antioxidant defense. *World Allergy Organization Journal*, 5(1), 9-19. <https://doi.org/10.1097/WOX.0b013e3182439613>
- Brandt, R., & Keston, A. S. (1965). Synthesis of diacetyldichlorofluorescein: A stable reagent for fluorometric analysis. *Analytical Biochemistry*, 11(1), 6-9. [https://doi.org/10.1016/0003-2697\(65\)90035-7](https://doi.org/10.1016/0003-2697(65)90035-7)
- Chang, C. T., Ho, T. Y., Lin, H., Liang, J. A., Huang, H. C., Li, C. C., Lo, H. Y., Wu, S. L., Huang, Y. F., & Hsiang, C. Y. (2012). 5-fluorouracil induced intestinal mucositis via nuclear factor- κ B activation by transcriptomic analysis and in vivo bioluminescence imaging. *PLoS ONE*, 7(3), e31808. <https://doi.org/10.1371/journal.pone.0031808>
- Costa, D. V. S., Bon-Frauches, A. C., Silva, A. M. H. P., Lima-Júnior, R. C. P., Martins, C. S., Leitão, R. F. C., Freitas, G. B., Castelucci, P., Bolick, D. T., Guerrant, R. L., Warren, C. A., Moura-Neto, V., & Brito, G. A. C. (2019). 5-Fluorouracil Induces Enteric Neuron Death and Glial Activation During Intestinal Mucositis via a S100B-RAGE-NF κ B-Dependent Pathway. *Scientific Reports*, 9(1), 1-14. <https://doi.org/10.1038/s41598-018-36878-z>
- Cuéllar-Garduño, N. (2015). Interacciones farmacológicas de la quimioterapia y la anestesia. *FARMACOLOGÍA EN ANESTESIA*, 38(1), S159–S162. <https://www.medigraphic.com/pdfs/rma/cma-2015/cmas151ai.pdf>
- El-Sayyad, H. I., Ismail, M. F., Shalaby, F. M., Abou-El-Magd, R. F., Gaur, R. L., Fernando, A., Raj, M. H. G., & Ouhtit, A. (2009). Histopathological effects of cisplatin, doxorubicin and 5-fluorouracil (5-FU) on the liver of male albino rats. *International Journal of Biological Sciences*, 5(5), 446. <https://doi.org/10.7150/ijbs.5.466>
- Ferlay J, Ervik M, Lam F, Colombet M, Mery L, Piñeros M, Znaor A, Soerjomataram I, B. F.

(2018). Global Cancer Observatory: Cancer Tomorrow. Lyon, France: International Agency for Research on Cancer. <https://gco.iarc.fr/tomorrow>

Gelen, V., Şengül, E., Yıldırım, S., & Atila, G. (2018). The protective effects of naringin against 5-fluorouracil-induced hepatotoxicity and nephrotoxicity in rats. *Iranian Journal of Basic Medical Sciences*, 21(4), 404. <https://doi.org/10.22038/ijbms.2018.27510.6714>

Harris, D. J. (2006). Cancer treatment-induced mucositis pain: Strategies for assessment and management. *Therapeutics and Clinical Risk Management*, 2(3), 251. <https://doi.org/10.2147/tcrm.2006.2.3.251>

Jiang, Z. Y., Woollard, A. C. S., & Wolff, S. P. (1991). Lipid hydroperoxide measurement by oxidation of Fe²⁺ in the presence of xylenol orange. Comparison with the TBA assay and an iodometric method. *Lipids*, 26(10), 853-856. <https://doi.org/10.1007/BF02536169>

Kang, K. A., Piao, M. J., Kim, K. C., Kang, H. K., Chang, W. Y., Park, I. C., Keum, Y. S., Surh, Y. J., & Hyun, J. W. (2014). Epigenetic modification of Nrf2 in 5-fluorouracil-resistant colon cancer cells: Involvement of TET-dependent DNA demethylation. *Cell Death and Disease*, 5(4), e1183. <https://doi.org/10.1038/cddis.2014.149>

Kubes, P., & McCafferty, D. M. (2000). Nitric oxide and intestinal inflammation. *American Journal of Medicine*, 109(2), 150-158. [https://doi.org/10.1016/S0002-9343\(00\)00480-0](https://doi.org/10.1016/S0002-9343(00)00480-0)

Leocádio, P. C. L., Antunes, M. M., Teixeira, L. G., Leonel, A. J., Alvarez-Leite, J. I., Machado, D. C. C., Generoso, S. V., Cardoso, V. N., & Correia, M. I. T. D. (2015). L-arginine pretreatment reduces intestinal mucositis as induced by 5-FU in mice, 67(3), 486-493. *Nutrition and Cancer*. <https://doi.org/10.1080/01635581.2015.1004730>

Marklund, S., & Marklund, G. (1974). Involvement of the superoxide anion radical in the autoxidation of pyrogallol and a convenient assay for superoxide dismutase. *Eur J Biochem*, 47(3), 469-474. <https://www.ncbi.nlm.nih.gov/pubmed/4215654>

McManus, J. F. A. (1946). Histological demonstration of mucin after periodic acid. *Nature*, 158(4006), 202. <https://doi.org/10.1038/158202a0>

McQuade, R. M., Stojanovska, V., Donald, E., Abalo, R., Bornstein, J. C., & Nurgali, K. (2016). Gastrointestinal dysfunction and enteric neurotoxicity following treatment with anticancer chemotherapeutic agent 5-fluorouracil. *Neurogastroenterology and Motility*, 28(120), 1861-1875. <https://doi.org/10.1111/nmo.12890>

Medeiros, A. da C., Azevedo, Í. M., Lima, M. L., Araújo Filho, I., & Moreira, M. D. (2018). Efeitos da sinvastatina na mucosite gastrointestinal induzida por 5-fluorouracil em ratos. *Revista Do Colégio Brasileiro de Cirurgiões*, 45(5), 1–8. <https://doi.org/10.1590/0100-6991e-20181968>

Muthu, R., Thangavel, P., Selvaraj, N., Ramalingam, R., & Vaiyapuri, M. (2013). Synergistic and individual effects of umbelliferone with 5-fluorouracil on the status of lipid peroxidation and antioxidant defense against 1, 2-dimethylhydrazine induced rat colon carcinogenesis. *Biomedicine and Preventive Nutrition*, 3(1), 74-82. <https://doi.org/10.1016/j.bionut.2012.10.011>

Okumura, R., & Takeda, K. (2017). Roles of intestinal epithelial cells in the maintenance of gut homeostasis. *Experimental and Molecular Medicine*, 49(5), e338. <https://doi.org/10.1038/emm.2017.20>

Pereira, A. S., Shitsuka, D. M., Parreira, F. J., & Shitsuka, R. (2018). Método Qualitativo, Quantitativo ou Quali-Quantitativo. In *Metodologia da Pesquisa Científica*. https://repositorio.ufsm.br/bitstream/handle/1/15824/Lic_Computacao_Metodologia-Pesquisa-Cientifica.pdf?sequence=1.

Prabhu, K. S., Reddy, P. V., Jones, E. C., Liken, A. D., & Reddy, C. C. (2004). Characterization of a class alpha glutathione-S-transferase with glutathione peroxidase activity in human liver microsomes. *Archives of Biochemistry and Biophysics*. <https://doi.org/10.1016/j.abb.2004.02.002>

Rivera, L. R., Thacker, M., Pontell, L., Cho, H. J., & Furness, J. B. (2011). Deleterious effects of intestinal ischemia/reperfusion injury in the mouse enteric nervous system are associated with protein nitrosylation. *Cell Tissue Res*, 344(1), 111–123. <https://doi.org/10.1007/s00441->

010-1126-x

Rtibi, K., Selmi, S., Grami, D., Amri, M., Sebai, H., & Marzouki, L. (2018). Contribution of oxidative stress in acute intestinal mucositis induced by 5 fluorouracil (5-FU) and its pro-drug capecitabine in rats. *Toxicology Mechanisms and Methods*, 28(4), 262-267. <https://doi.org/10.1080/15376516.2017.1402976>

Sedlak, J., & Lindsay, R. H. (1968). Estimation of total, protein-bound, and nonprotein sulfhydryl groups in tissue with Ellman's reagent. *Anal Biochem*, 25(1), 192-205. <https://www.ncbi.nlm.nih.gov/pubmed/4973948>

Shiota, A., Hada, T., Baba, T., Sato, M., Yamanaka-Okumura, H., Yamamoto, H., Taketani, Y., & Takeda, E. (2010). Protective effects of glyco glycerol lipids extracted from spinach on 5-fluorouracil induced intestinal mucosal injury. *Journal of Medical Investigation*. https://www.jstage.jst.go.jp/article/jmi/57/3,4/57_3,4_314/_article/-char/ja/

Sies, H. (1999). Glutathione and its role in cellular functions. *Free Radical Biology and Medicine*. [https://doi.org/10.1016/S0891-5849\(99\)00177-X](https://doi.org/10.1016/S0891-5849(99)00177-X)

Soares, P. M. G., Mota, J. M. S. C., Gomes, A. S., Oliveira, R. B., Assreuy, A. M. S., Brito, G. A. C., Santos, A. A., Ribeiro, R. A., & Souza, M. H. L. P. (2008). Gastrointestinal dysmotility in 5-fluorouracil-induced intestinal mucositis outlasts inflammatory process resolution. *Cancer Chemotherapy and Pharmacology*. <https://doi.org/10.1007/s00280-008-0715-9>

Soares, P. M. G., Mota, J. M. S. C., Souza, E. P., Justino, P. F. C., Franco, A. X., Cunha, F. Q., Ribeiro, R. A., & Souza, M. H. L. P. (2013). Inflammatory intestinal damage induced by 5-fluorouracil requires IL-4. *Cytokine*. <https://doi.org/10.1016/j.cyto.2012.10.003>

Sonis, S. T., Elting, L. S., Keefe, D., Peterson, D. E., Schubert, M., Hauer-Jensen, M., Bekele, B. N., Raber-Durlacher, J., Donnelly, J. P., & Rubenstein, E. B. (2004). Perspectives on cancer therapy-induced mucosal injury. *Cancer*, 100(S9), 1995-2025. <https://doi.org/10.1002/cncr.20162>

Tiwari, V; Kuhad, A; Chopra, K. (2011). Emblica officinalis corrige déficits funcionais, bioquímicos e moleculares na neuropatia diabética experimental, visando a cascata inflamatória mediada pelo estresse oxido-nitrosativo. *Phytother. Res*, 25, 1527–1536. <https://doi.org/10.1002/ptr.3440>

Warholm, M., Guthenberg, C., von Bahr, C., & Mannervik, B. (1985). Glutathione transferases from human liver. *Methods Enzymol*, 113, 499–504. <https://www.ncbi.nlm.nih.gov/pubmed/3003505>

Yasuda, M., Kato, S., Yamanaka, N., Iimori, M., Matsumoto, K., Utsumi, D., Kitahara, Y., Amagase, K., Horie, S., & Takeuchi, K. (2013). 5-HT₃ receptor antagonists ameliorate 5-fluorouracil-induced intestinal mucositis by suppression of apoptosis in murine intestinal crypt cells. *British Journal of Pharmacology*. <https://doi.org/10.1111/bph.12019>

Percentage of contribution of each author in the manuscript

Lilian Catarim Fabiano - 30%

Mariana Conceição da Silva - 7%

Karile Cristina da Costa - 7%

Pedro Luiz Zonta de Freitas - 7%

Camila Quaglio Neves - 7%

Stephanie Carvalho Borges - 7%

Ana Cristina Breithaupt-Faloppa - 5%

Nilza Cristina Buttow - 30%